



Assessment of laboratory O₄ absorption cross-sections at 360 nm using atmospheric long-path DOAS observations

Bianca Lauster^{1,2}, Udo Frieß², Jan-Marcus Nasse^{2,3}, Ulrich Platt², and Thomas Wagner^{1,2}

¹Satellite Remote Sensing Group, Max Planck Institute for Chemistry, Mainz, Germany

²Institute for Environmental Physics, University of Heidelberg, Heidelberg, Germany

³Now at: Energie Baden-Württemberg AG, Karlsruhe, Germany

Correspondence: Bianca Lauster (b.lauster@mpic.de)

Abstract. The atmospheric absorption of the oxygen collision complex O₂-O₂, in the following referred to as O₄, can be used to derive properties of aerosols and clouds from remote sensing observations. In recent years, inconsistencies between the measured atmospheric O₄ absorption and radiative transfer simulations were found for Multi-AXis Differential Optical Absorption Spectroscopy (MAX-DOAS) measurements. In the presented study, over two years of observations from a long-path (LP-) DOAS instrument deployed at the German research station Neumayer, Antarctica, are analysed. While MAX-DOAS instruments measure spectra of scattered sunlight at different elevation angles, LP-DOAS utilises an artificial light source and the atmospheric absorptions are measured along a fixed (and well-defined) light path close to the surface. Further, the pristine measurement location allows to investigate the relation between measured and modelled O₄ absorption over a large range of temperatures (-45°C to +5°C). Overall good agreement is found between the retrieved O₄ absorption cross-sections covering the absorption band at 360 nm and laboratory measurements. While the best agreement is obtained for the Finkenzeller and Volkamer (2022) cross-sections, deviations at cold ambient temperatures (below ca. -25°C) are observed for the Thalman and Volkamer (2013) cross-sections. Other O₄ absorption bands could not be investigated because these are not (fully) within the spectral range of the measured spectra. This study strongly supports the accuracy of commonly used O₄ absorption cross-sections in DOAS analyses, while more work is needed to understand the earlier reported inconsistencies in MAX-DOAS observations.

1 Introduction

Atmospheric absorption of the oxygen collision complex O₂-O₂ (in the following referred to as O₄) in the UV-visible spectral range is commonly used in remote sensing applications to derive properties of aerosol and clouds. The atmospheric concentration of O₄ is proportional to the square of the O₂ concentration. Deviations from the O₄ absorption against those for clear sky conditions thus indicate changes in atmospheric radiative transfer which allows to retrieve properties of cloud and/or aerosol particles from such observations. This technique can be applied to remote sensing measurements of scattered sunlight performed by ground-based instruments, airborne platforms and satellites (e.g., Hönninger et al., 2004; Wagner et al., 2004, 2010; Wittrock et al., 2004; Frieß et al., 2006, 2016; Irie et al., 2008; Prados-Roman et al., 2011).



Over a decade ago, Wagner et al. (2009) first reported inconsistencies between the measured atmospheric O₄ absorption
25 from Multi-AXis Differential Optical Absorption Spectroscopy (MAX-DOAS) observations and radiative transfer simulations.
MAX-DOAS instruments measure scattered sunlight under various mostly slant elevation angles (Hönninger et al., 2004). To
achieve agreement with the forward model simulations, Wagner et al. (2009) suggested applying a scaling factor (SF < 1) to
the measured O₄ slant column densities (SCDs). Similar findings were then reported by, e.g., Clémer et al. (2010), Vlemmix
et al. (2015), Frieß et al. (2016) and Wagner et al. (2021), who all found best agreement for SF between 0.75 and 0.9, while
30 other studies (including direct sun measurements and aircraft measurements) did not see the necessity for a scaling factor (e.g.,
Spinei et al., 2015; Ortega et al., 2016).

A more detailed overview and discussion can be found in Wagner et al. (2019). Since there is still no consensus in the
community on whether or not an SF is appropriate, this ambiguity leads to substantial uncertainties in the aerosol results
derived from MAX-DOAS measurements.

35 In this study, long-term long-path (LP-) DOAS observations are used to examine the O₄ absorption between 352 and 387 nm
covering the absorption band at 360 nm. The absorption band at 577 nm is not fully covered leading to a less stable retrieval
and thus was excluded from a more detailed investigation. The different analyses include the commonly used absorption cross-
sections of Thalman and Volkamer (2013) as well as Finkenzeller and Volkamer (2022) at different temperatures. Figure 1
shows the respective cross-sections at 293 K and the wavelength range covered by the data.

40 At first, differences between MAX-DOAS and LP-DOAS measurements are detailed in the next section answering the
question why LP-DOAS observations are well suited to further investigate the reported inconsistencies from MAX-DOAS
studies. After the following description of the measurement set-up and analysis, the main part focuses on the comparison
between measured and calculated O₄ absorptions. Lastly, the findings of this study are summarised and put into the context of
previous and future work.

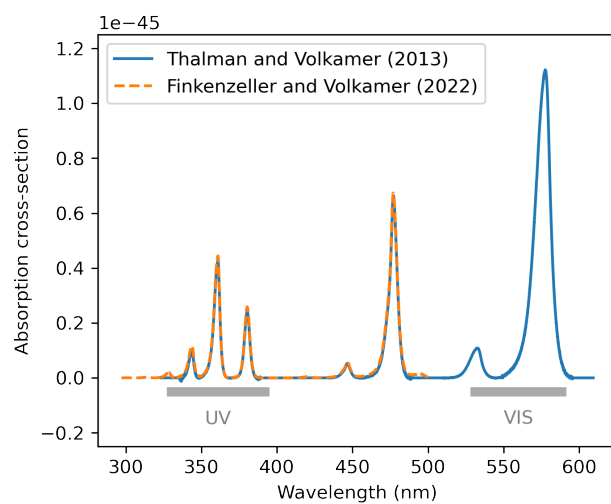


Figure 1. O₄ absorption cross-sections investigated in this study. The grey bars indicate the wavelength range measured by the LP-DOAS instrument. Note that the absorption band at 477 nm is not covered by the measurements. The figure depicts the absorption cross-sections at 293 K.



45 2 Long-path DOAS

2.1 Suitability for accurate atmospheric O₄ absorption measurements

Long-path (LP-) DOAS belongs to the active DOAS applications (Perner et al., 1976; Perner and Platt, 1980; Platt and Perner, 1983) and is a well-established remote sensing technique. In contrast to passive systems which measure scattered sunlight, such as MAX-DOAS instruments, LP-DOAS instruments use artificial light sources, for example a Xenon arc lamp or in more recent applications a laser driven light source. Thereby, continuous observations of trace gases are possible independent of natural light sources, i.e., also during night-time and in the deep UV. The most prominent advantage for the presented study is the well-defined light path of a LP-DOAS set-up. Along this light path, a mean trace gas concentration is determined. In MAX-DOAS analyses, the conversion from SCDs to concentrations always requires further processing steps including radiative transfer simulations and thus possibly leads to a higher uncertainty of the results. Also direct sun measurements, despite the well-defined light path, experience further difficulties such as small atmospheric absorptions. Another benefit of LP-DOAS measurements is that the ambient temperature and pressure can be assumed constant along the given light path of a couple of kilometres at ground level, while this is not the case in MAX-DOAS retrievals or direct sun measurements which measure the vertical column density and therefore have to consider temperature and pressure vertical profiles. Nonetheless, the basis of the DOAS principle is applicable to both active and passive DOAS systems.

60 2.2 Instrument and measurement site

The LP-DOAS instrument used in this study was purpose-built for operation under polar conditions. Its observations complement the long-term measurements at the German research station Neumayer III, Antarctica, from January 2016 to August 2018. A detailed description of the instrument and its set-up can be found in Nasse et al. (2019) and Nasse (2019).

The LP-DOAS instrument couples light from a laser driven light source into a telescope located at the trace gas observatory of the Neumayer III station (Fig. 2) which creates a light beam that is transmitted through the atmosphere across a distance of 1.55 km (Met retro) or 2.95 km (Atka retro). Depending on the prevailing weather conditions, the amount of reflected light varies between the two retro-reflectors and the shorter light path can be chosen for difficult atmospheric conditions with lower visibility. After reflection at one of the retro-reflector arrays, the light is received again by the same telescope doubling the length of the light path. The measured spectra are analysed based on the DOAS principle. Details of the analysis are given in the next section.

The measurement site exhibits an extraordinarily large temperature range exceeding -35°C and +0°C as can be seen in Fig. 3. Apart from seasonal variations, these temperatures are driven by the advection of air masses of different origin, depending on synoptic conditions. The annual cycle of surface pressure indicates the influence of large scale atmospheric patterns around the Antarctic continent (König-Langlo et al., 1998).

Given its remote location, the aerosol optical depth is often below 0.1 (see, e.g., respective site on the AERONET webpage, NASA-GSFC) making the station an ideal location for this study. In particular, the majority of the measurement days exhibit an only slightly attenuated signal after passing the atmospheric light path twice.

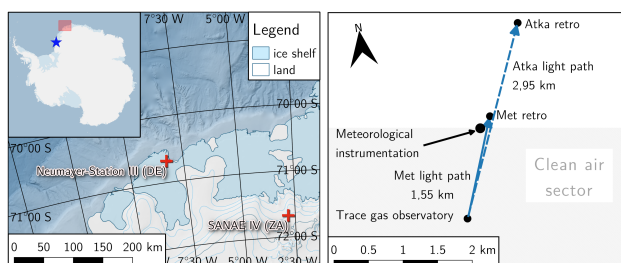


Figure 2. Location of the Neumayer III station on the Ekström ice shelf (left) and overview of the installations in the vicinity of the station (right). The closest neighbouring station is the South African base SANAE IV about 225 km to the south-east, while the British station Halley VI (blue star) is the only other Antarctic station located on an ice shelf and about 800 km south-west of Neumayer III (Schiermeier, 2004). Taken from Nasse (2019).

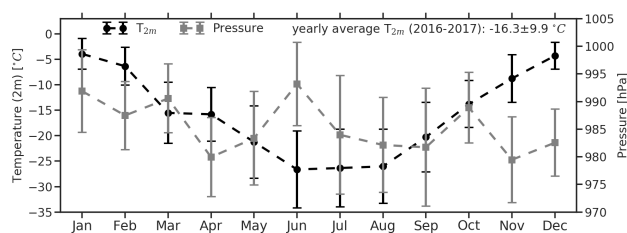


Figure 3. Monthly averages of 2 m temperature and atmospheric pressure at the Neumayer III station. For details, see Nasse (2019). The whiskers indicate one standard deviation of the data. Taken from Nasse (2019).



2.3 Data analysis

Average trace gas concentrations along the light path can be retrieved for each measured spectrum by making use of the Lambert-Beer law. For atmospheric applications, this is commonly referred to as the DOAS approach (Platt and Stutz, 2008). In the study presented here, the spectral analysis of the obtained spectra is performed in HeiDOAS (v1.2). This newly developed Python-based library was programmed for the analysis of DOAS measurements and conducts the fit using a Levenberg-Marquardt algorithm (Levenberg, 1944; Marquardt, 1963) allowing for the commonly used parameters in DOAS analyses.

While MAX-DOAS applications usually use zenith measurements as a reference, the LP-DOAS instrument can measure an absorption-free spectrum of the light source by moving a reference plate into the light path and thereby creating a short-cut for the light. To determine and correct the influence of the atmospheric background as well as instrumental contributions of the dark current signal from the CCD and the electronic offset, regular background spectra are recorded in addition by shutting off the light source. The wavelength calibration is accomplished by determining the channel-to-wavelength attribution from measurements of emission line spectra of a mercury and a neon vapour lamp. These calibration spectra were recorded regularly throughout the measurement campaign and also allow to retrieve the instrumental slit function needed for the convolution of the fitted absorption cross-sections.

After the preprocessing of the data, i.e. conducting the wavelength calibration and accounting for the background, the measured spectra are fitted according to the DOAS fit settings given in Table 1. In order to remove broad-band spectral features that are caused by the light source or the optical components and can have characteristic shapes, a binomial high-pass filter and a low order closure polynomial is applied. Different analyses will be shown in the following including one O_4 absorption cross-section as stated.

To account for quickly varying atmospheric conditions between the acquisition of the atmospheric spectrum and the respective background spectrum, an atmospheric background spectrum is also included in the DOAS fit which becomes important if the background correction cannot fully compensate for the background signal.

Figure 4 exemplarily shows a fit in the UV spectral range with the clearly visible O_4 absorption. On the contrary, in the visible spectral range the absorption band of the oxygen collision complex is not fully covered leading to a less stable retrieval as can be seen from Fig. A1 in the appendix. Additionally, strong water vapour absorption features lead to higher residuals. Altogether, this demonstrates the challenges of LP-DOAS data analysis in the visible spectral range for which reason the following study focuses on the UV retrieval. Assuring good data quality, fits are filtered for a root-mean-squares (RMS) of the residual of less than 2×10^{-4} .

During the analysis, it was found that modifications of the applied binomial high-pass filter (HP) can influence the retrieved O_4 column densities which was thus studied more carefully. The variation of other fit settings, e.g., the choice of fitted cross-sections or in-/excluding an atmospheric background spectrum in the fit, has small impact compared to the choice of the high-pass filter.

Systematic differences of the measured spectra, e.g., arising from broad-band spectral variations caused by the reflectivity of the short-cut plate, require the application of a high-pass filter since the correction of the spectral features arising from



115 these differences is hardly possible by the usage of a polynomial only (Pöhler, 2010). Also, the cut-off frequency between narrow- and broad-band absorptions is well-defined by the width of the binomial kernel of the high-pass filter. Note that the filter is defined inversely, i.e. the smaller the width the stronger the filtering effect. For instance, the filters' full width at half maximum correspond to 2.5 nm, 3.5 nm and 4.3 nm for the high-pass filters applying 4000, 8000 (standard) and 12000 iterations, respectively, given the spectral dispersion of 68.7 nm to 2048 channels. The variation of the cut-off frequency leads to a relative difference in the retrieved O_4 column densities well below 5% and mainly an enhanced scatter of the values in case of a too strong filter (HP 4000) as can be seen from Fig. 5.



Table 1. DOAS fit settings for the “standard” analysis in the UV spectral range.

Fit range	352 – 387 nm
Polynomial	3
High-pass filter	4000
Cross-sections	BrO (228 K; Wilmouth et al., 1999) NO ₂ (294 K; Vandaele et al., 1998) O ₃ (243 K; Serdyuchenko et al., 2014) O ₄ (various; Thalman and Volkamer, 2013; Finkenzeller and Volkamer, 2022) Atmospheric background
Shift & stretch	Applied to spectrum wavelengths

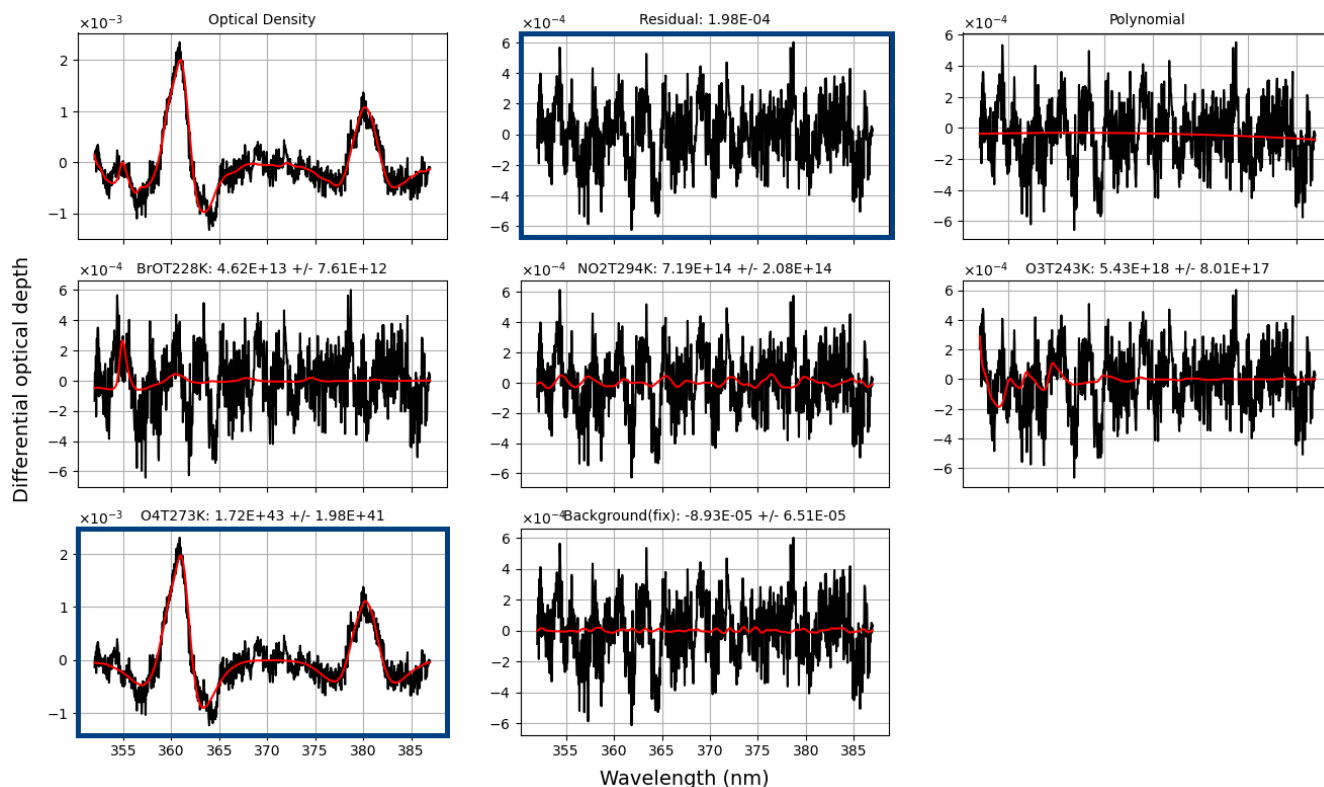


Figure 4. Example fit in the UV. The optical density panel depicts the logarithm of the high-pass filtered ratio of measured atmospheric spectrum and its respective reference, i.e., short-cut spectrum. The residual as well as the fitted O_4 are highlighted by the blue boxes. The remaining panels show the other fitted cross-sections as given in the title (red) and the fit plus residuum (black). The titles additionally name the temperature at which each absorption cross-section was measured and the retrieved column density in molec cm^{-2} (in the case of O_4 : molec $^2 cm^{-5}$).

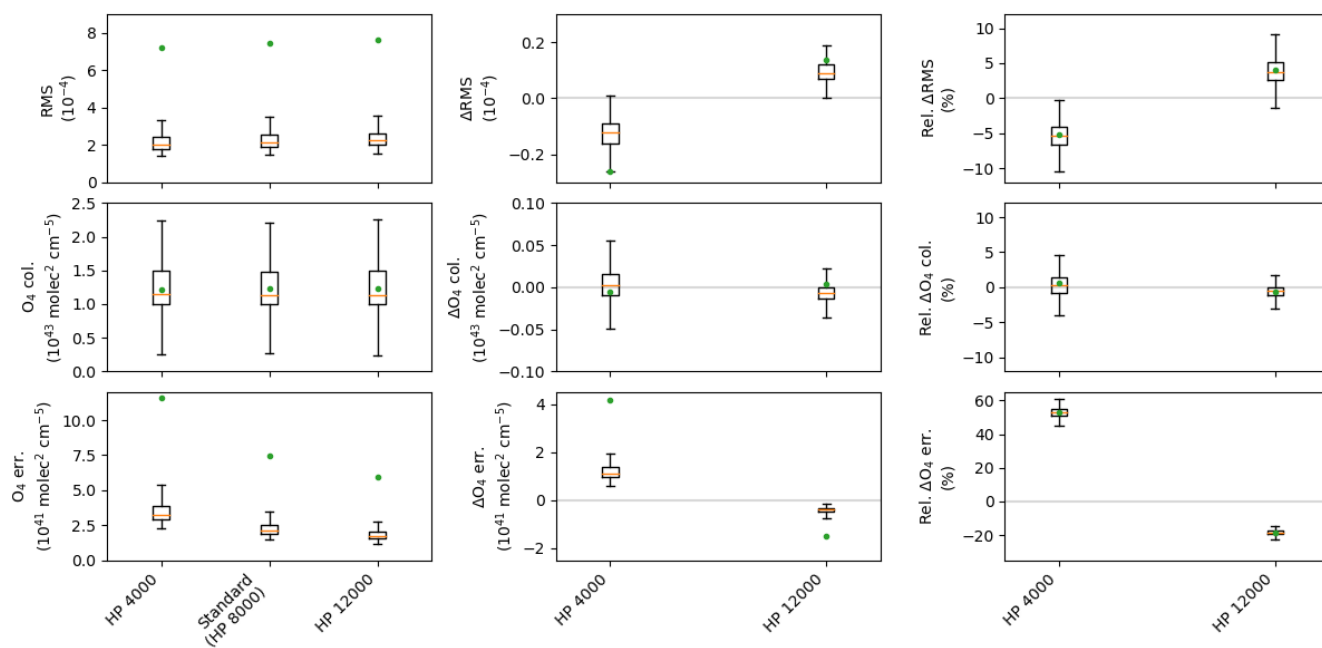


Figure 5. RMS, retrieved O₄ column and fit error in box-whisker-plots for the standard fit settings (as given in Table ??) as well as fit settings with a high-pass filter (HP) of 12000 and 4000 iterations as indicated in the label (left column). Absolute and relative differences to the standard retrieval are shown for all three quantities in the middle and right column, respectively. Each box extends from the lower to upper quartile values of the data (interquartile range, IQR), with an orange line at the median. The mean value is represented by a green dot. The whiskers extend to 1.5×IQR from the edges of the box, ending at the farthest data point within that interval.



3 Comparison between measured and calculated O₄ concentrations

120 3.1 Set-up of the comparison study

First, the measured O₄ column densities are converted into O₄ concentrations by dividing by the light path length which can easily be done since the light path for LP-DOAS measurements is well-defined. Given the fact that the O₄ concentration is proportional to the square of the O₂ concentration in the atmosphere, the expected O₄ concentrations can be computed via the ideal gas law

$$125 \quad pV = Nk_B T$$

where p is the pressure, V the volume, N the number of particles, k_B the Boltzmann constant and T the temperature. Rearranging the formula yields the O₄ concentration

$$c_{O_4} \propto (c_{O_2})^2 = \left(0.21 \times \frac{p}{k_B T}\right)^2.$$

130 Since the equilibrium constant ($2O_2 \leftrightarrow O_4$) is unknown, the unit of the O₄ “concentration” is molec² cm⁻⁶. However, the common O₄ absorption cross-sections are scaled accordingly such that a direct comparison to the squared O₂ concentration is possible. The expected O₄ concentration is then calculated for each time of a spectral measurement by inserting the respective pressure and temperature values from the meteorological long-term observations at the measurement site (Schmithüsen, 2023).

Figure 6 shows the correlation of measured and calculated O₄ concentrations for the complete data set covering over two years of data (January 2016 to August 2018) and a temperature range of more than 35 K. In total, more than 69000 spectra
135 were analysed. The DOAS analysis was carried out with the fit settings as given in Table 1 in the UV spectral range using the Thalman and Volkamer (2013) absorption cross-section at 253 K. Assuming that best agreement is found for an ambient temperature of the O₄ absorption cross-section, i.e., in this case at 253 K, and taking into consideration the slight pressure differences during the measurement period, the best agreement between measured and calculated values is expected where indicated by the grey bar. However, mostly slight overestimations of the computed O₄ concentrations are observed within
140 the shaded area. Generally, the retrieval yields too low O₄ values at higher temperatures and too high O₄ values at lower temperatures indicating the importance of the temperature dependence of the O₄ absorption.

To investigate the temperature dependence of the cross-sections (i.e., the strength of its peak value), analyses are done not only with the Thalman and Volkamer (2013) absorption cross-section at 253 K but also other available temperatures as well as the newer absorption cross-sections by Finkenzeller and Volkamer (2022). The corresponding results are summarised in
145 Fig. A2 and A3 in the appendix.

It can be seen that the usage of the Thalman and Volkamer (2013) absorption cross-section at 233 K yields too low O₄ concentrations even for temperatures around 233 K (compare grey bar, upper left plot in Fig. A2). For the absorption cross-sections at 273 K and 293 K, good agreement for measurements at the respective temperatures is found. Overall, the O₄ absorption cross-sections by Thalman and Volkamer (2013) show a non-linear temperature dependence with larger deviations for
150 low-temperature cross-sections.



This finding is in accordance to the change of the spectral bands' shapes or in other words the decrease of the peak values of the O_4 absorption cross-sections with temperature, which are particularly important to DOAS observations, while the integrated absorption cross-sections are independent of temperatures Thalman and Volkamer (2013).

155 Similar results are obtained for the analyses including Finkenzeller and Volkamer (2022) absorption cross-sections. Here, the temperature dependence of the cross-sections seems to be weaker and especially at low temperatures a better agreement to the calculated O_4 concentrations is observed.

Basically identical results are found for both O_4 absorption cross-sections at 293 K from Thalman and Volkamer (2013) and from Finkenzeller and Volkamer (2022) (compare lowermost panels in Fig. A2 and A3), respectively.

160 All in all, these results indicate a good agreement between measured and calculated O_4 concentrations for LP-DOAS measurements in the UV spectral range. Still some deviations at ambient temperatures other than those corresponding to the temperature of the used absorption cross-section are found. To eliminate these, an interpolated O_4 absorption cross-section could be used as will be detailed in the next section.

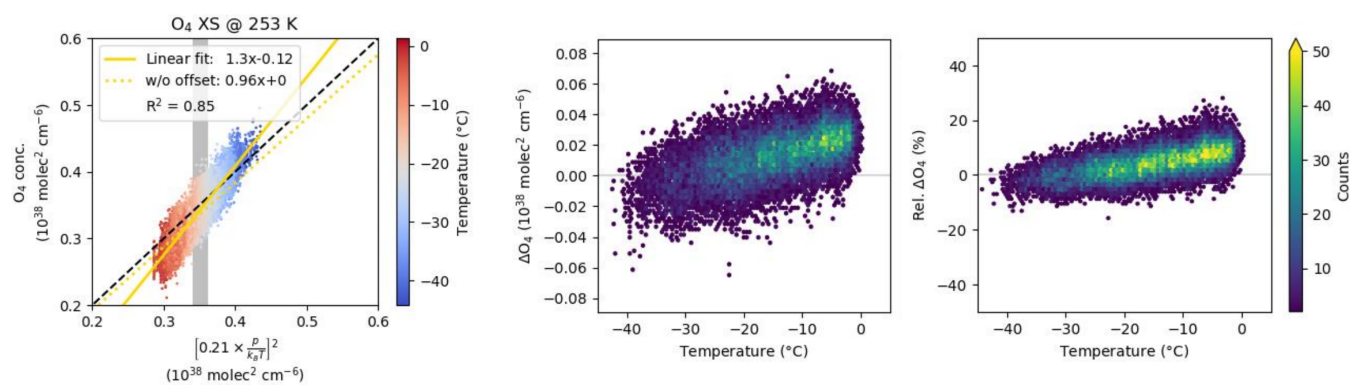


Figure 6. Correlation of measured O₄ concentrations using a fixed absorption cross-section (from Thalman and Volkamer, 2013, at 253 K, corresponding to -20°C) (ordinate) to values calculated from ambient temperature and pressure (abscissa). Details on the retrieval and calculation are given in the main text. The grey bar indicates the range where for the chosen cross-section at 253 K best agreement between measured and calculated values is expected. Fit parameters of a linear fit with and without (w/o) intercept as well as the correlation coefficient are given in the legend. Data points are colour-coded for the respective temperature during the measurement. The middle and right panels show the absolute and relative difference between the measured O₄ concentration and the calculated values with regard to temperature, respectively.



3.2 Usage of interpolated O₄ absorption cross-sections

The advantage of LP-DOAS observations with collocated temperature measurements is the exact knowledge of the ambient
165 temperature for each spectrum acquisition. Thus, the best matching O₄ absorption cross-section can be chosen individually for
each spectrum during the DOAS retrieval. However, the absorption cross-sections are only available for a couple of specific
temperatures (namely at 203, 233, 253, 273 and 293 K for Thalman and Volkamer, 2013; 223, 263 and 293 K for Finkenzeller
and Volkamer, 2022). In order to match a given temperature, the set of available cross-sections is linearly interpolated to fit the
required temperature. This newly calculated interpolated O₄ absorption cross-section is then used in the DOAS fit.

170 Using these interpolated O₄ absorption cross-sections leads to a clear improvement in the comparison between measured and
computed O₄ concentrations for the Thalman and Volkamer (2013) as well as Finkenzeller and Volkamer (2022) cross-sections.
The results are shown in Fig. 7 and 8, respectively. As already noted, largest discrepancies exist for the Thalman and Volkamer
(2013) version at low ambient temperatures (below ca. -25°C) indicating that the peak values of the O₄ absorption cross-section
at low temperatures is too large. On the contrary, the interpolated version of Finkenzeller and Volkamer (2022) cross-sections
175 shows nearly perfect agreement for the entire temperature range with a mean difference of only $0.006 \times 10^{38} \text{ molec}^2 \text{ cm}^{-5}$ and
a slope of the data close to 1 (compare golden lines in Fig. 8).

This demonstrates the consistency between the O₄ absorption cross-sections from Finkenzeller and Volkamer (2022) mea-
sured under laboratory conditions and real atmospheric measurements.

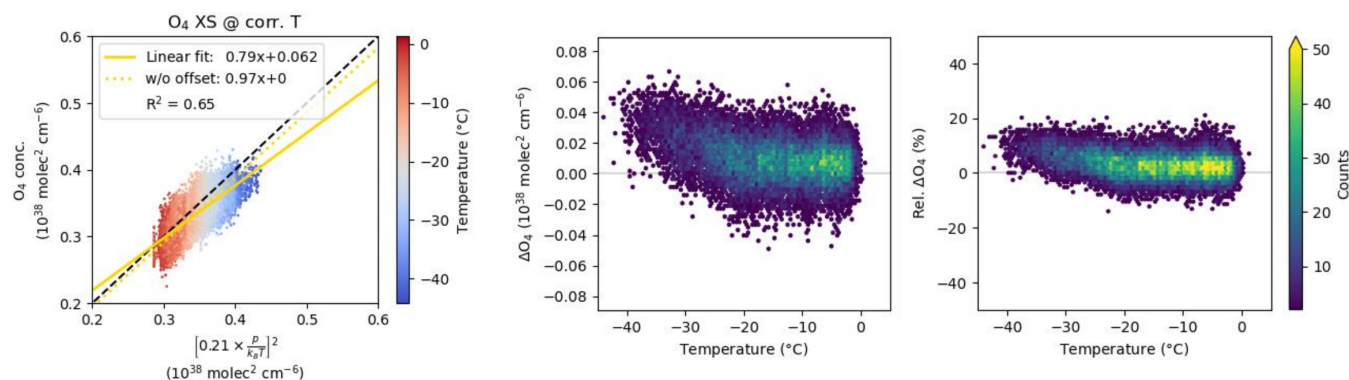


Figure 7. Correlation of measured O_4 concentrations using an interpolated absorption cross-section based on all Thalman and Volkamer (2013) cross-sections to calculated values. Details on the retrieval and calculation are given in the main text. For the plot description, see Fig. 6.

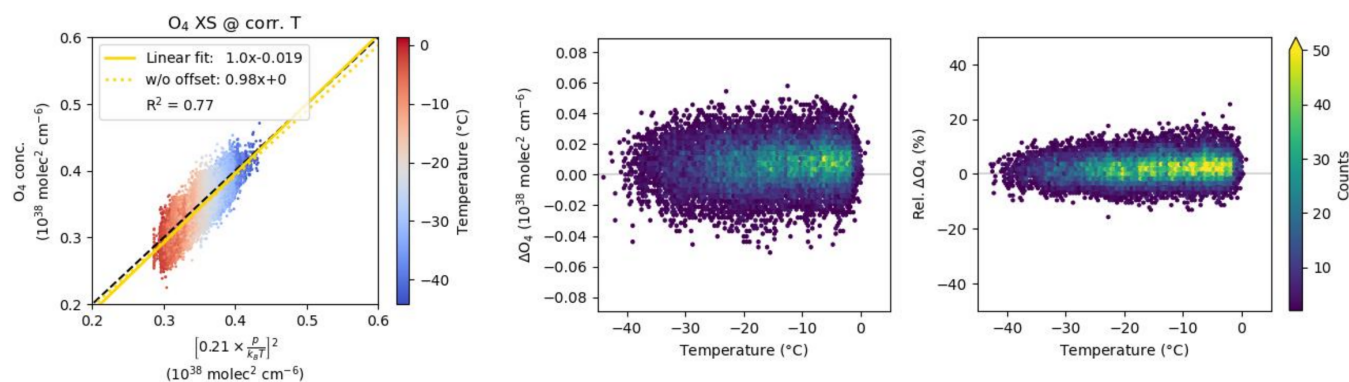


Figure 8. Correlation of measured O_4 concentrations using an interpolated absorption cross-section based on all Finkenzeller and Volkamer (2022) cross-sections to calculated values. Details on the retrieval and calculation are given in the main text. For the plot description, see Fig. 6.



4 Conclusions and outlook

180 The comparison of measured and calculated O_4 concentrations shows a good agreement of the O_4 absorption from atmospheric LP-DOAS observations with the commonly used O_4 absorption cross-sections measured under laboratory conditions when properly accounting for the temperature dependence of the O_4 absorption. Thereby, the DOAS analysis was run for the spectral range from 352 to 387 nm covering the strong absorption band at 360 nm. Best agreement was found for the recently published O_4 absorption cross-sections of Finkenzeller and Volkamer (2022) and the approach of an interpolated O_4 absorption
185 cross-section fitting to the ambient temperature of the measurements. The retrieval using the Thalman and Volkamer (2013) absorption cross-sections show larger than expected O_4 concentrations at low temperatures (below ca. -25°C).

This study shows that the need for a scaling factor in MAX-DOAS profile inversions is not caused by a possible systematic error of the available O_4 absorption cross-sections, but leaves the problem of the O_4 scaling factor yet unresolved. Many other hypotheses have already been tested, e.g., in Wagner et al. (2019) and Wagner et al. (2021). These studies included the
190 investigation of the temperature dependence of the O_4 absorption and temperature variations along the light path of MAX-DOAS measurements, but concluded that this alone cannot explain the observed discrepancies.

Therefore, further work is needed to understand why an O_4 scaling factor becomes necessary in some MAX-DOAS retrievals, while this is not the case for LP-DOAS data. It should include a direct comparison of LP-DOAS and MAX-DOAS observations at the Neumayer III station, which was, however, beyond the scope of this study. Also, additional LP-DOAS
195 measurements covering the 477 nm absorption band as well as an improved retrieval for spectra in the visible spectral range could help to enhance the understanding of the O_4 scaling factor. Lastly, it should be considered to repeat some of the previous studies with the newer O_4 absorption cross-sections of Finkenzeller and Volkamer (2022).

Code and data availability. Long-path DOAS data and analysis software are available upon request from the corresponding author. The auxiliary data are freely accessible online (see references in main text).

200 Appendix A: Additional tables and figures



Table A1. DOAS fit settings for the analysis in the visible spectral range.

Fit range	550 – 585 nm
Polynomial	3
High-pass filter	none
Cross-sections	H ₂ O (293 K; Lampel et al., 2015) NO ₂ (294 K; Vandaele et al., 1998) O ₃ (243 K; Serdyuchenko et al., 2014) O ₄ (various; Thalman and Volkamer, 2013)
	Atmospheric background
Shift & stretch	Applied to spectrum wavelengths

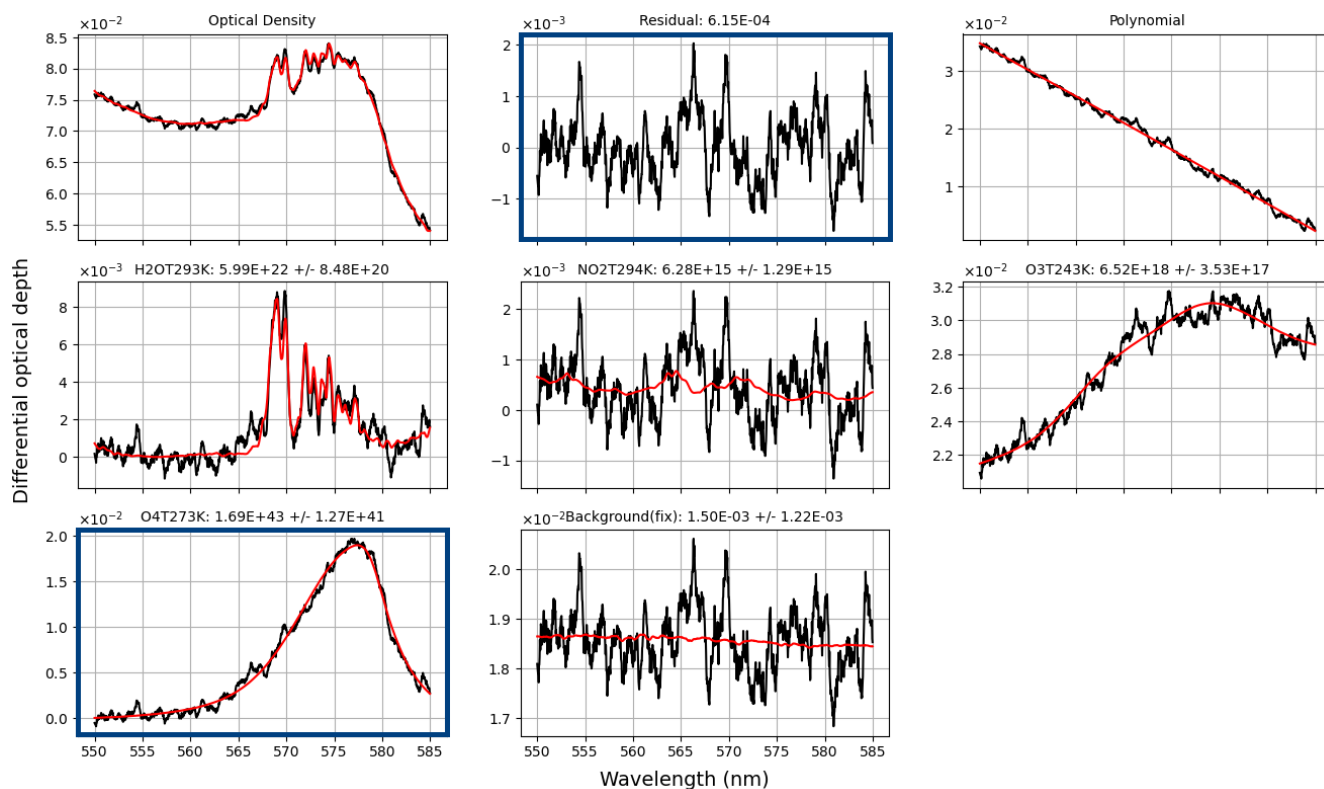


Figure A1. Example fit in the visible spectral range using the fit settings given in Table A1. For the plot description, see Fig. 4.

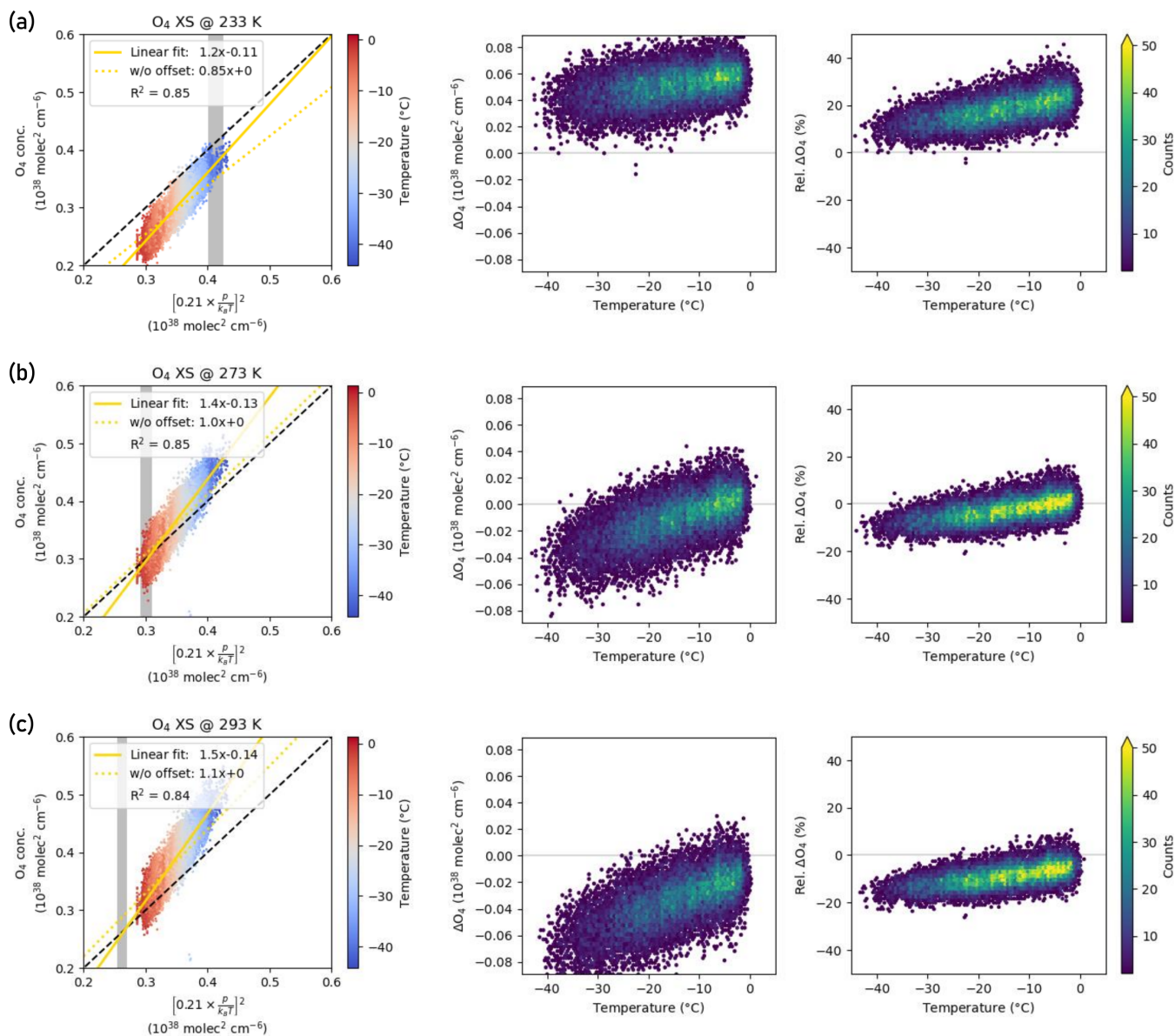


Figure A2. Same as Fig. 6 but for the Thalman and Volkamer (2013) absorption cross-sections at 223 K (a), 273 K (b) and 293 K (c).

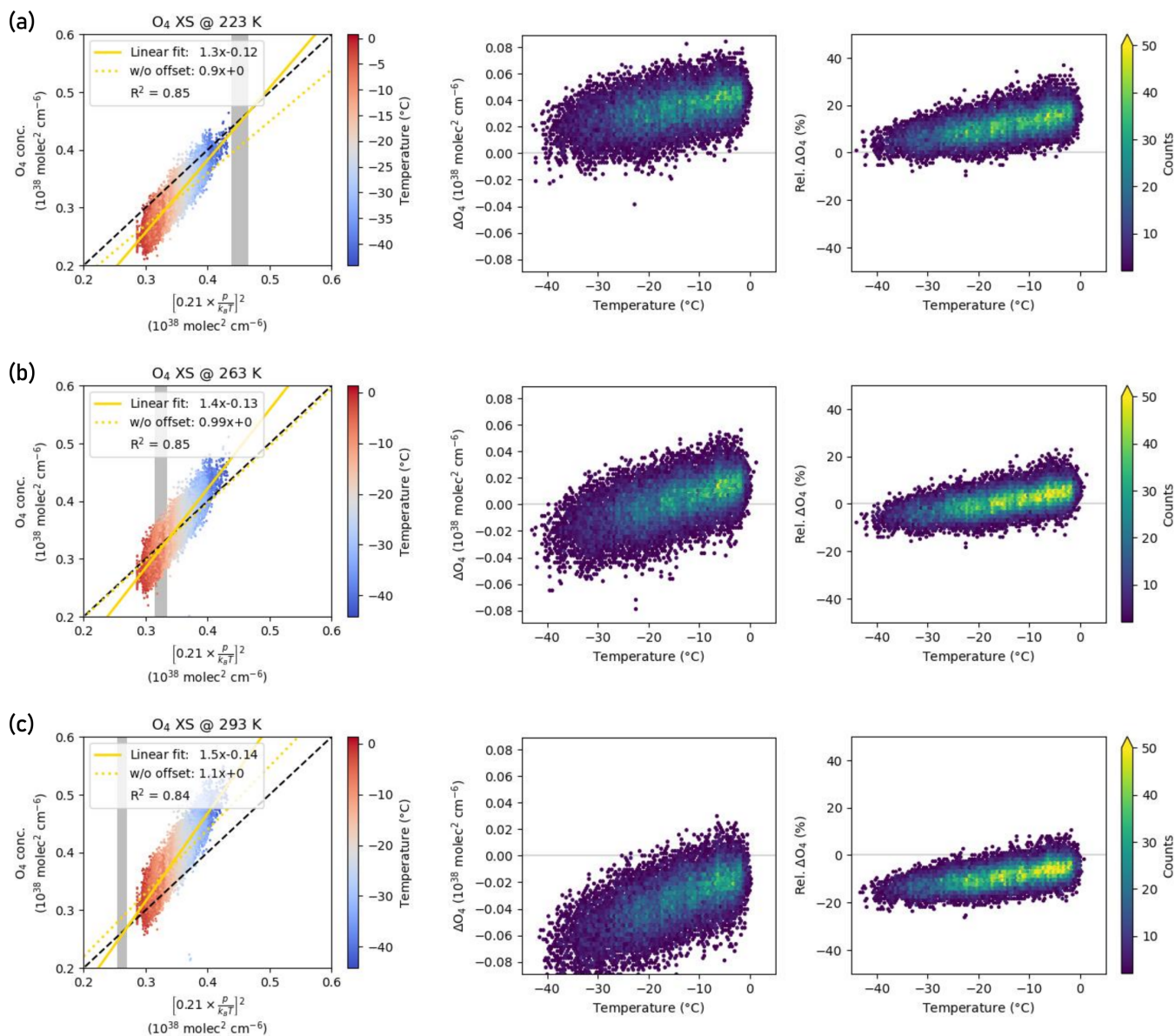


Figure A3. Same as Fig. 6 but for the Finkenzeller and Volkamer (2022) absorption cross-sections at 233 K (a), 263 K (b) and 293 K (c).



Author contributions. BL and TW designed the study. BL run the data analysis with support by UF and interpreted the results together with TW, UP and UF. JN and UF designed the LP-DOAS instrument and performed the measurements in Antarctica. UF developed the heiDOAS analysis software. BL prepared the manuscript with contributions from all co-authors.

Competing interests. At least one of the (co-)authors is a member of the editorial board of *Atmospheric Measurement Techniques*.

205 *Acknowledgements.* We acknowledge the workshop of IUP Heidelberg and all involved people for the thorough construction of the LP-
DOAS instrument. Special thanks goes to Denis Pöhler and Stefan Schmitt who were involved in the planning, design and set-up of the
LP-DOAS instrument. Furthermore, we thank Dr. Rolf Weller and colleagues of the Alfred Wegener Institute that made it possible to acquire
this data set at the Antarctic research station Neumayer III. In particular, we acknowledge the air chemists Thomas Schaefer, Zsófia Jurányi
and Helene Hoffmann as well as the entire 36th, 37th and 38th wintering crews that stayed at the Neumayer station and kept the LP-DOAS
210 running throughout all weather conditions.

Financial support. Measurements at Neumayer III have been supported by the Deutsche Forschungsgesellschaft (DFG) in the framework of
the project HALOPOLE III (grant no. FR 2497/3-2).



References

- Clémer, K., Van Roozendaal, M., Fayt, C., Hendrick, F., Hermans, C., Pinardi, G., Spurr, R., Wang, P., and De Mazière, M.: Multiple
215 wavelength retrieval of tropospheric aerosol optical properties from MAXDOAS measurements in Beijing, *Atmospheric Measurement
Techniques*, 3, 863–878, <https://doi.org/10.5194/amt-3-863-2010>, 2010.
- Finkenzeller, H. and Volkamer, R.: O₂–O₂ CIA in the gas phase: Cross-section of weak bands, and continuum absorption between
297–500 nm, *Journal of Quantitative Spectroscopy and Radiative Transfer*, 279, 108 063, <https://doi.org/10.1016/j.jqsrt.2021.108063>,
2022.
- 220 Frieß, U., Monks, P. S., Remedios, J. J., Rozanov, A., Sinreich, R., Wagner, T., and Platt, U.: MAX-DOAS O₄ measurements: A new
technique to derive information on atmospheric aerosols: 2. Modeling studies, *Journal of Geophysical Research: Atmospheres*, 111,
<https://doi.org/10.1029/2005jd006618>, 2006.
- Frieß, U., Klein Baltink, H., Beirle, S., Clémer, K., Hendrick, F., Henzing, B., Irie, H., de Leeuw, G., Li, A., Moerman, M. M., van Roozen-
dael, M., Shaiganfar, R., Wagner, T., Wang, Y., Xie, P., Yilmaz, S., and Zieger, P.: Intercomparison of aerosol extinction profiles retrieved
225 from MAX-DOAS measurements, *Atmospheric Measurement Techniques*, 9, 3205–3222, <https://doi.org/10.5194/amt-9-3205-2016>, 2016.
- Hönninger, G., von Friedeburg, C., and Platt, U.: Multi axis differential optical absorption spectroscopy (MAX-DOAS), *Atmospheric Chem-
istry and Physics*, 4, 231–254, <https://doi.org/10.5194/acp-4-231-2004>, 2004.
- Irie, H., Kanaya, Y., Akimoto, H., Iwabuchi, H., Shimizu, A., and Aoki, K.: First retrieval of tropospheric aerosol profiles us-
ing MAX-DOAS and comparison with lidar and sky radiometer measurements, *Atmospheric Chemistry and Physics*, 8, 341–350,
230 <https://doi.org/10.5194/acp-8-341-2008>, 2008.
- König-Langlo, G., King, J. C., and Pettré, P.: Climatology of the three coastal Antarctic stations Dumont d’Urville, Neumayer, and Halley,
Journal of Geophysical Research: Atmospheres, 103, 10 935–10 946, <https://doi.org/10.1029/97jd00527>, 1998.
- Lampel, J., Pöhler, D., Tschirter, J., Frieß, U., and Platt, U.: On the relative absorption strengths of water vapour in the blue wavelength
range, *Atmospheric Measurement Techniques*, 8, 4329–4346, <https://doi.org/10.5194/amt-8-4329-2015>, 2015.
- 235 Levenberg, K.: A method for the solution of certain non-linear problems in least squares, *Quarterly of Applied Mathematics*, 2, 164–168,
<https://doi.org/10.1090/qam/10666>, 1944.
- Marquardt, D. W.: An Algorithm for Least-Squares Estimation of Nonlinear Parameters, *Journal of the Society for Industrial and Applied
Mathematics*, 11, 431–441, <https://doi.org/10.1137/0111030>, 1963.
- NASA-GSFC: AERONET (Aerosol Robotic Network), <https://aeronet.gsfc.nasa.gov/>, last updated: August 06, 2024.
- 240 Nasse, J.-M.: Halogens in the coastal boundary layer of Antarctica, phdthesis, Universität Heidelberg,
<https://doi.org/10.11588/HEIDOK.00026489>, 2019.
- Nasse, J.-M., Eger, P. G., Pöhler, D., Schmitt, S., Frieß, U., and Platt, U.: Recent improvements of long-path DOAS measurements: impact
on accuracy and stability of short-term and automated long-term observations, *Atmospheric Measurement Techniques*, 12, 4149–4169,
<https://doi.org/https://doi.org/10.5194/amt-12-4149-2019>, 2019.
- 245 Ortega, I., Berg, L. K., Ferrare, R. A., Hair, J. W., Hostetler, C. A., and Volkamer, R.: Elevated aerosol layers modify the O₂–O₂
absorption measured by ground-based MAX-DOAS, *Journal of Quantitative Spectroscopy and Radiative Transfer*, 176, 34–49,
<https://doi.org/10.1016/j.jqsrt.2016.02.021>, 2016.
- Perner, D. and Platt, U.: Absorption of light in the atmosphere by collision pairs of oxygen (O₂)₂, *Geophysical Research Letters*, 7, 1053–
1056, <https://doi.org/10.1029/gl007i012p01053>, 1980.



- 250 Perner, D., Ehhalt, D. H., Pätz, H. W., Platt, U., Röth, E. P., and Volz, A.: OH - Radicals in the lower troposphere, *Geophysical Research Letters*, 3, 466–468, <https://doi.org/10.1029/gl003i008p00466>, 1976.
- Platt, U. and Perner, D.: Measurements of Atmospheric Trace Gases by Long Path Differential UV/Visible Absorption Spectroscopy, pp. 97–105, Springer Berlin Heidelberg, ISBN 9783540395522, https://doi.org/10.1007/978-3-540-39552-2_13, 1983.
- Platt, U. and Stutz, J.: *Differential Optical Absorption Spectroscopy: Principles and Applications*, Springer Science & Business Media, ISBN 9783540757764, <https://doi.org/10.1007/978-3-540-75776-4>, 2008.
- 255 Prados-Roman, C., Butz, A., Deutschmann, T., Dorf, M., Kritten, L., Minikin, A., Platt, U., Schlager, H., Sihler, H., Theys, N., Van Roozendaal, M., Wagner, T., and Pfeilsticker, K.: Airborne DOAS limb measurements of tropospheric trace gas profiles: case studies on the profile retrieval of O₄ and BrO, *Atmospheric Measurement Techniques*, 4, 1241–1260, <https://doi.org/10.5194/amt-4-1241-2011>, 2011.
- Pöhler, D.: Determination of two dimensional trace gas distributions using tomographic LP-DOAS measurements in the city of Heidelberg, Germany, phdthesis, Universität Heidelberg, 2010.
- 260 Schiermeier, Q.: Cold comfort, *Nature*, 431, 734–735, <https://doi.org/10.1038/431734a>, 2004.
- Schmithüsen, H.: Continuous meteorological observations at Neumayer station (1982-03 et seq), <https://doi.org/10.1594/PANGAEA.962313>, 2023.
- Serdyuchenko, A., Gorshchev, V., Weber, M., Chehade, W., and Burrows, J. P.: High spectral resolution ozone absorption cross-sections – Part 2: Temperature dependence, *Atmospheric Measurement Techniques*, 7, 625–636, <https://doi.org/10.5194/amt-7-625-2014>, 2014.
- 265 Spinei, E., Cede, A., Herman, J., Mount, G. H., Eloranta, E., Morley, B., Baidar, S., Dix, B., Ortega, I., Koenig, T., and Volkamer, R.: Ground-based direct-sun DOAS and airborne MAX-DOAS measurements of the collision-induced oxygen complex, O₂O₂, absorption with significant pressure and temperature differences, *Atmospheric Measurement Techniques*, 8, 793–809, <https://doi.org/10.5194/amt-8-793-2015>, 2015.
- 270 Thalman, R. and Volkamer, R.: Temperature dependent absorption cross-sections of O₂–O₂ collision pairs between 340 and 630 nm and at atmospherically relevant pressure, *Physical Chemistry Chemical Physics*, 15, 15 371, <https://doi.org/10.1039/c3cp50968k>, 2013.
- Vandaele, A., Hermans, C., Simon, P., Carleer, M., Colin, R., Fally, S., Mérimée, M., Jenouvrier, A., and Coquart, B.: Measurements of the NO₂ absorption cross-section from 42 000 cm⁻¹ to 10 000 cm⁻¹ (238–1000 nm) at 220 K and 294 K, *Journal of Quantitative Spectroscopy and Radiative Transfer*, 59, 171–184, [https://doi.org/10.1016/s0022-4073\(97\)00168-4](https://doi.org/10.1016/s0022-4073(97)00168-4), 1998.
- 275 Vlemmix, T., Hendrick, F., Pinardi, G., De Smedt, I., Fayt, C., Hermans, C., PETERS, A., Wang, P., Levelt, P., and Van Roozendaal, M.: MAX-DOAS observations of aerosols, formaldehyde and nitrogen dioxide in the Beijing area: comparison of two profile retrieval approaches, *Atmospheric Measurement Techniques*, 8, 941–963, <https://doi.org/10.5194/amt-8-941-2015>, 2015.
- Wagner, T., Dix, B., Friedeburg, C. v., Frieß, U., Sanghavi, S., Sinreich, R., and Platt, U.: MAX-DOAS O₄ measurements: A new technique to derive information on atmospheric aerosols—Principles and information content, *Journal of Geophysical Research: Atmospheres*, 109, <https://doi.org/10.1029/2004jd004904>, 2004.
- 280 Wagner, T., Deutschmann, T., and Platt, U.: Determination of aerosol properties from MAX-DOAS observations of the Ring effect, *Atmospheric Measurement Techniques*, 2, 495–512, <https://doi.org/10.5194/amt-2-495-2009>, 2009.
- Wagner, T., Beirle, S., Deutschmann, T., and Penning de Vries, M.: A sensitivity analysis of Ring effect to aerosol properties and comparison to satellite observations, *Atmospheric Measurement Techniques*, 3, 1723–1751, <https://doi.org/10.5194/amt-3-1723-2010>, 2010.
- 285 Wagner, T., Beirle, S., Benavent, N., Bösch, T., Chan, K. L., Donner, S., Dörner, S., Fayt, C., Frieß, U., García-Nieto, D., Gielen, C., González-Bartolome, D., Gomez, L., Hendrick, F., Henzing, B., Jin, J. L., Lampel, J., Ma, J., Mies, K., Navarro, M., Peters, E., Pinardi, G., Puentedura, O., Pukite, J., Remmers, J., Richter, A., Saiz-Lopez, A., Shaiganfar, R., Sihler, H., Van Roozendaal, M., Wang, Y., and



- 290 Yela, M.: Is a scaling factor required to obtain closure between measured and modelled atmospheric O₄ absorptions? An assessment of uncertainties of measurements and radiative transfer simulations for 2 selected days during the MAD-CAT campaign, *Atmospheric Measurement Techniques*, 12, 2745–2817, <https://doi.org/10.5194/amt-12-2745-2019>, 2019.
- Wagner, T., Dörner, S., Beirle, S., Donner, S., and Kinne, S.: Quantitative comparison of measured and simulated O₄ absorptions for one day with extremely low aerosol load over the tropical Atlantic, *Atmospheric Measurement Techniques*, 14, 3871–3893, <https://doi.org/10.5194/amt-14-3871-2021>, 2021.
- 295 Wilmouth, D. M., Hanisco, T. F., Donahue, N. M., and Anderson, J. G.: Fourier Transform Ultraviolet Spectroscopy of the A 2Π_{3/2} ← X 2Π_{3/2} Transition of BrO, *The Journal of Physical Chemistry A*, 103, 8935–8945, <https://doi.org/10.1021/jp991651o>, 1999.
- Wittrock, F., Oetjen, H., Richter, A., Fietkau, S., Medeke, T., Rozanov, A., and Burrows, J. P.: MAX-DOAS measurements of atmospheric trace gases in Ny-Ålesund - Radiative transfer studies and their application, *Atmospheric Chemistry and Physics*, 4, 955–966, <https://doi.org/10.5194/acp-4-955-2004>, 2004.